



Effect of H_3PO_3 concentration on the electrodeposition of nanocrystalline Ni–P deposited in an emulsified supercritical CO_2 bath

Sung-Ting Chung, Yan-Chi Chuang, Shih-Yi Chiu, Wen-Ta Tsai*

Department of Materials Science and Engineering, National Cheng Kung University, Tainan, Taiwan

ARTICLE INFO

Article history:

Received 8 August 2011

Received in revised form 1 October 2011

Accepted 1 October 2011

Available online 14 October 2011

Keywords:

Electrodeposition

Supercritical CO_2

Ni–P deposits

Nanocrystalline

ABSTRACT

The electrodeposition of Ni–P alloy in an emulsified supercritical carbon dioxide (sc-CO_2) bath was investigated to explore the effect of H_3PO_3 concentration (ranging from 0 to 1.6 M) on the material characteristics of the deposits. The experimental results showed that the P content in the deposit increased with increasing H_3PO_3 concentration in the emulsified sc-CO_2 bath, while the weight gain of the Ni–P film decreased. At the same concentration of H_3PO_3 , the significant decreases in weight gain and P content of the Ni–P films deposited in the emulsified sc-CO_2 bath were found, as compared with that plated in the conventional aqueous electrolyte at ambient pressure. X-ray photoelectron analyses revealed that the carbon-containing Ni–P deposit could be obtained in the bath with the presence of sc-CO_2 fluid. Transmission electron microscopy was employed for microstructure analysis. The average grain size of the Ni–P films deposited in the conventional aqueous electrolyte at ambient pressure or in the emulsified sc-CO_2 bath varied, depending on the H_3PO_3 concentration and P content. The Ni–P films deposited from the emulsified sc-CO_2 bath had a higher hardness as compared with that formed in conventional electrolyte. The hardness of Ni–P alloy deposited in the emulsified sc-CO_2 bath was enhanced by the additional solid solution strengthening mechanism.

© 2011 Elsevier Ltd. All rights reserved.

1. Introduction

Ni–P films have been widely used as hard coatings owing to their satisfactory mechanical properties, reasonable cost and ease of manufacturing [1–3]. Numerous studies have been devoted to the fabrication of Ni–P alloy films using electrodeposition and electroless deposition methods [4–6]. Electrodeposition processes are less expensive, have faster deposition rates, and more stable baths than electroless deposition [6]. Despite their different deposition mechanisms, the electrodeposition and electroless deposition of Ni–P alloys all lead to higher micro-hardness values than the pure Ni. It has been shown that most of the properties of electrodeposited nickel are structure-dependent, and that the structure is closely related to the P content of the deposits [7]. The explanations proposed for the increase in micro-hardness include solid solution hardening, precipitation hardening, and grain size strengthening [8–10]. The effect of deposition parameters, such as solution pH, current density and the concentration of H_3PO_3 on composition, structure and mechanical properties of Ni–P electrodeposits has been studied extensively [1,10–16]. Deposits with high P content ($\text{P} > 7 \text{ wt.}\%$) exhibit an amorphous structure. However, the extreme brittleness and high sensitivity to notch with the high P alloys

overshadow their advantages [14,15], and low P alloys ($\text{P} < 7 \text{ wt.}\%$) with nanocrystalline grains have thus attracted research attention.

Furthermore, the substitution of toxic electrolytes with environmentally friendly ones is vitally important to minimize environmental pollution. Recently, several researchers [17–19] have begun to develop a new method for electrodeposition in a bath involving supercritical CO_2 (sc-CO_2), and our previous studies [20–22] also showed that the Ni deposited in such a bath had low surface roughness, small grain size, high micro-hardness, and high corrosion resistance. We also found that the fine grain size and solid solution strengthening due to carbon were responsible for the higher hardness observed.

In order to further improve the mechanical performance of Ni film, P addition in the Ni matrix was attempted in this investigation by an electrodeposition process in an emulsified sc-CO_2 bath. The corresponding material and mechanical properties were examined systematically. The Ni/P content ratio was controlled by adjusting the H_3PO_3 concentration in the modified deposition solution, and an improvement in the hardness of the Ni coating due to the introduction of P element was found.

2. Experimental

A brass sheet with a surface area of $2 \text{ cm} \times 2.4 \text{ cm}$ was used as the cathode for electrodeposition. Each substrate was successively ground with SiC paper to a grit of #2000, followed by polishing

* Corresponding author. Tel.: +886 6 275 7575x62927; fax: +886 6 275 4395.
E-mail address: wtsai@mail.ncku.edu.tw (W.-T. Tsai).

Table 1
Bath composition and conditions used for Ni–P electrodeposition.

Electrolyte	Concentration	Deposition conditions	
		Parameters	Value
NiSO ₄ ·6H ₂ O	120 g/L	Current density	2 A/dm ²
NiCl ₂ ·6H ₂ O	20 g/L	Bath temperature	50 °C
H ₃ BO ₃	15 g/L	Deposition time	90 min
Citric acid	15 g/L	Solution pH	3.0
Saccharin	1 g/L		
C ₇ H ₉ NO ₂ S	0.5 g/L	Conventional electrolyte (exposed to air)	0.1 MPa
H ₃ PO ₃	0–1.6 M	Electrolyte in Ar gas	10 MPa
C ₁₂ EO ₈	0.1 vol.%	Electrolyte in sc-CO ₂	10 MPa

with Al₂O₃ slurry to 0.3 μm, degreased in 0.1 M NaOH solution and followed by water rinsing, etched in 0.1 M H₂SO₄ solution, rinsed with de-ionized water, and finally dried using a stream of hot air.

A high pressure cell made of stainless steel, with a volume of 650 mL, was fabricated for the electroplating in a bath containing sc-CO₂ fluid. The electroplating system has been described elsewhere [20]. Two types of electrodeposition baths, namely conventional and emulsified sc-CO₂, were used in this investigation. The conventional one consisted of 120 g/L NiSO₄·6H₂O, 20 g/L NiCl₂·6H₂O, 15 g/L H₃BO₃, 15 g/L citric acid, 1 g/L saccharin, 0.5 g/L C₇H₉NO₂S and various concentrations of H₃PO₃ (ranging from 0 to 1.6 M). When the conventional bath was used, electrodeposition was conducted either at ambient pressure or at 10 MPa under Ar atmosphere. The emulsified sc-CO₂ bath was prepared by purging pressurized CO₂ at 10 MPa into the conventional bath with proper addition of C₁₂EO₈ surfactant to ensure an emulsified fluid was attained. The bath consisted of 350 mL of the above aqueous solution and 300 mL of sc-CO₂ fluid. The composition of the bath and the operating conditions employed in this investigation are listed in Table 1. Electroplating was performed under constant current density conditions at 2 A/dm² for 90 min.

After electroplating, material characterization was performed. The chemical composition of the Ni–P alloy was measured by energy dispersive spectrometry (EDS). The crystal structure of the as-plated film was analyzed by X-ray diffraction (XRD, Rigaku Mini-FlexII) using monochromatic Cu Kα (λ = 1.540562 nm) radiation. X-ray photoelectron spectroscopy (XPS, PHI 5000 VersaProbe) was carried out using Al Kα excitation with a fixed analyzer transmission of 117.4 and 23.5 eV pass energy, 1 and 0.2 eV step size for survey and high-resolution spectra, respectively. The microstructure of the nickel films was observed with a transmission electron microscope (TEM, FEI Tecnai G2 20 S-Twin) with an emission voltage of 200 kV. The hardness measurements were carried out using a nano-indenter equipped with a diamond tip. The loading was applied at a strain rate of 0.05/s till a penetration depth of 1000 nm. The corresponding hardness was then determined. The average of five readings was taken as the hardness value of each Ni–P film.

3. Results and discussion

3.1. Weight gain

The weight gains of pure Ni and Ni–P alloy films electrodeposited both in conventional aqueous electrolyte at ambient pressure and in the emulsified sc-CO₂ bath with various concentrations of H₃PO₃ were measured. As shown in Fig. 1, the weight gain of the deposits decreased with increasing H₃PO₃ concentration in both baths. The weight gain of the Ni–P deposit formed in the conventional bath with 0.35 M of H₃PO₃ under an Ar atmosphere of 10 MPa was also determined. The result was the same as that formed at ambient pressure, suggesting the insignificant effect of pressure on the electrodeposition behavior in the conventional bath.

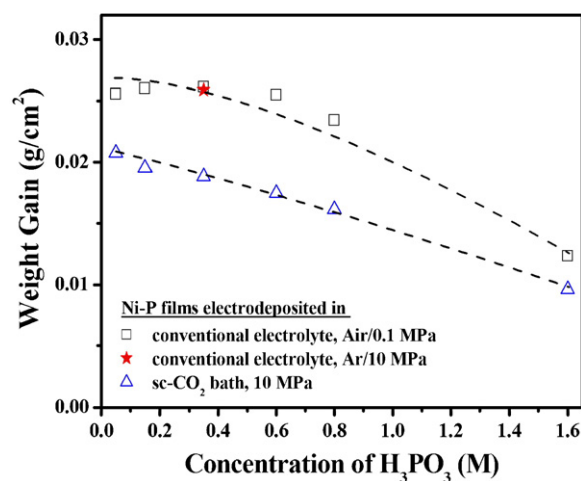
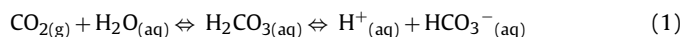


Fig. 1. Weight gain of Ni–P films electrodeposited in the conventional electrolyte containing different H₃PO₃ concentrations at ambient pressure, in Ar atmosphere at 10 MPa, and in the emulsified sc-CO₂ bath at 10 MPa.

In the emulsified sc-CO₂ bath at 10 MPa, the weight gain of the electrodeposited Ni–P film was lower than that formed in aqueous electrolyte at ambient pressure, as shown in Fig. 1. The characteristics of emulsion between water and supercritical carbon dioxide, as addressed by many researchers [23,24], could play important role in electroplating. In this emulsified bath, based on the work of Sone and his co-workers [25], the formation of micelle (either CO₂ in H₂O or H₂O in CO₂) caused a reduction in the number of active sites at the substrate/electrolyte interface for electrochemical reactions. As a result, the deposition rate was hindered and the weight gain mainly associated with Ni and/or P reductions was lower as compared with that performed in the conventional bath. The lower conductivity of the emulsified sc-CO₂ bath, as pointed out by Kim et al. [26], was also responsible for the lower weight gain observed. In addition, the lower pH value of the aqueous electrolyte could be maintained through the formation of carbonic acid by dissolving carbon dioxide in water following the chemical reaction [10,27]:



Previous studies [21,28,29] had also demonstrated the effect of solution pH via the above reaction in affecting the electrodeposition of Ni and the electroless Ni–B deposition, respectively. The adsorption of HCO₃[−] on the deposit surface might also retard the reduction of Ni²⁺, leading to a lower current efficiency observed in the emulsified sc-CO₂ bath.

The cross-section micrographs of the Ni–P alloy films electrodeposited in the conventional and the emulsified sc-CO₂ baths are shown in Fig. 2. With a deposition time of 90 min at 2 A/dm², the thickness of the deposit formed in the emulsified sc-CO₂ bath was 17 μm, thinner than that electrodeposited in the conventional aqueous electrolyte (25 μm). Obviously, the deposition rate in the

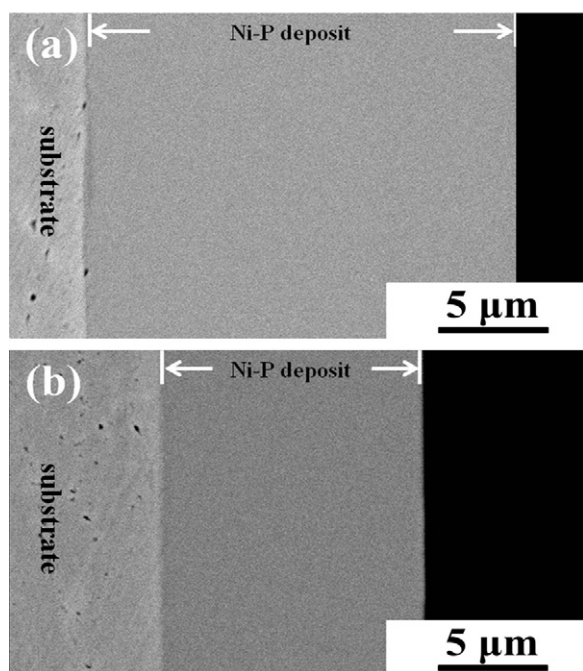


Fig. 2. Cross-section micrographs of the Ni–P films electrodeposited in the conventional electrolyte containing 0.35 M H_3PO_3 at 2 A/dm^2 for 90 min (a) at ambient pressure (0.1 MPa) and (b) in the emulsified sc- CO_2 bath at 10 MPa.

emulsified sc- CO_2 bath was lower than that found in the conventional bath, and these results are consistent with the weight gain measurements.

3.2. Chemical composition analysis

3.2.1. P content in the as deposited Ni–P alloy films

EDS was employed to determine the P content in the deposit. The variation of P content with H_3PO_3 concentration is demonstrated in Fig. 3. For deposits formed in the conventional bath at ambient pressure, P content increased from 4.6 to 24.9 at.%, with increasing H_3PO_3 concentration from 0.05 to 1.6 M. By applying an Ar atmosphere of 10 MPa to the bath containing 0.35 M H_3PO_3 , the P content in the deposit (about 9.7 at.%) was almost the same as that formed at ambient pressure. The results indicate that the P content in the Ni–P deposit formed in the conventional bath is independent of the applied pressure.

Table 2

P content, grain size, and hardness of Ni–P films electrodeposited in conventional electrolyte containing different H_3PO_3 concentrations at ambient pressure and in the sc- CO_2 bath at 10 MPa.

Condition of coating	$[\text{H}_3\text{PO}_3]$ (M)	P content (at.%)	Grain size (nm)	Hardness (GPa)	
Conventional electrolyte 0.1 MPa	Ni deposit	0	43	5.2	
		0.05	37	8.2	
		0.15	22	7.8	
	Ni–P deposit	0.35	9.7	9	9.0
		0.6	14.4	7	10.3
		0.8	20.9	4	9.3
1.6		25.0	3	8.8	
Sc- CO_2 bath 10 MPa	Ni deposit	0	17	9.5	
		0.05	18	12.1	
		0.15	3.7	16	12.0
	Ni–P deposit	0.35	4.9	14	12.4
		0.6	5.7	12	12.5
		0.8	6.5	13	12.0
		1.6	7.7	11	11.9

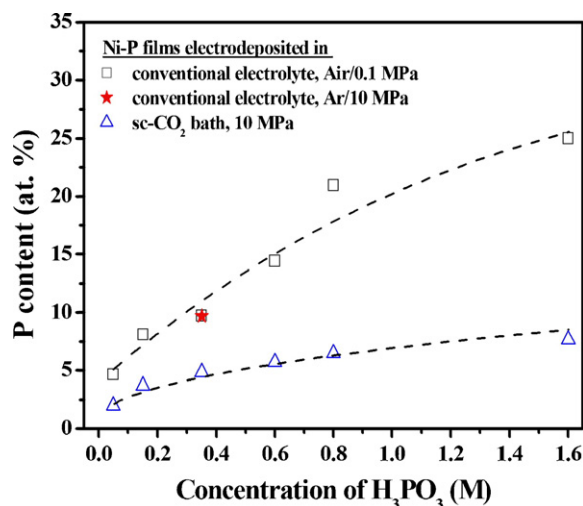


Fig. 3. P content in the Ni–P films electrodeposited in the conventional electrolyte containing different H_3PO_3 concentrations at ambient pressure, in Ar atmosphere at 10 MPa, and in the emulsified sc- CO_2 bath at 10 MPa.

Similar results were found for the Ni–P films deposited in the emulsified sc- CO_2 bath. The P content in the deposit increased from 2.0 to 7.7 at.% with increasing H_3PO_3 concentration from 0.05 to 1.6 M. The results shown in Fig. 3 clearly reveal that the Ni–P films deposited in the emulsified sc- CO_2 bath had a lower P content than those formed in the conventional bath with the same H_3PO_3 concentration. The P content in the Ni–P alloy layers formed in a conventional bath at ambient pressure and in that containing sc- CO_2 is shown in Table 2. The retardation of P co-deposition with the presence of sc- CO_2 fluid was significant, which was attributed to the co-deposition of carbon, as will be discussed later.

3.2.2. XPS analysis

XPS was employed for chemical composition analysis of the Ni–P deposits. Before the analysis, each Ni or Ni–P film was cleaned by Ar^+ ion etching for 1 min. The C1s spectra for the Ni–P film deposited in the bath with or without sc- CO_2 fluid are shown in Fig. 4. The absence of C1s in the Ni–P film deposited in conventional bath at ambient pressure indicates that Ar^+ ion etching was adequate for surface cleaning to eliminate any C contamination. For the Ni–P film deposited in the conventional aqueous electrolyte under an Ar atmosphere of 10 MPa, a similar result (without discernible C1s peak) was obtained. For the Ni–P film electrodeposited in the emulsified sc- CO_2 bath, a distinct C1s peak was observed,

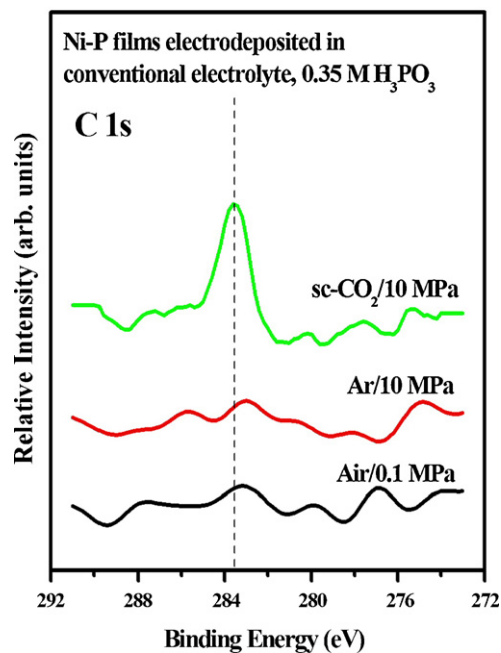
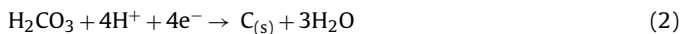


Fig. 4. X-ray photoelectron spectra of the C1s region of Ni–P films electrodeposited in the conventional electrolyte containing 0.35 M H_3PO_3 at ambient pressure, in Ar atmosphere at 10 MPa, and in the emulsified sc- CO_2 bath at 10 MPa, after Ar^+ sputtering to remove atmospheric contaminants.

as shown in Fig. 4. The C1s binding energy obtained in this case was 283.6 eV, close to that for graphitic carbon (284.6 eV) [30]. The small deviation from the graphitic carbon C1s binding energy was due to the formation of metal–carbon bonds, as has been reported elsewhere [21,31,32]. In the electrolyte containing sc- CO_2 fluid, as described in this investigation, the formation of Ni–P deposit could be accompanied by the following reaction:



Electro-carburization of Ni in the system incorporating sc- CO_2 fluid has been reported in our previous studies [21,22]. The XPS results obtained in this investigation further confirmed the alloying of carbon into Ni–P film electrodeposited in the emulsified sc- CO_2 bath. Since the electro-carburization described in reaction (2) is a reduction reaction which competes for electrons, therefore, the amounts of Ni and P reduced from the electrolyte under constant charges in the bath containing sc- CO_2 are less than those in the conventional bath, as revealed in Figs. 1 and 3.

3.3. Crystal structure

The XRD patterns of the Ni–P coatings prepared in the conventional bath at ambient pressure and in the emulsified sc- CO_2 bath, both with different H_3PO_3 concentrations, are illustrated in Figs. 5 and 6, respectively. As shown in Fig. 5, pure Ni (P free) electrodeposited in the conventional bath was crystalline and exhibited a face-centered cubic structure with a preferred crystallographical plane of (200). In the bath containing 0.35 M H_3PO_3 , an obvious change of the preferred crystallographical plane from (200) to (111) was observed. As the H_3PO_3 concentration was further increased to 0.8 M, the diffraction peak intensity decreased significantly, indicating the loss of crystallinity. At 1.6 M H_3PO_3 , the diffraction peak almost disappeared, implying the formation of an amorphous phase in the electrodeposit. The effect of P on the change of crystal structure has been addressed elsewhere [33–35]. Owing to the different atomic radii, the alloying of P causes a distortion of the base Ni lattices. As the P content increases, the lattice

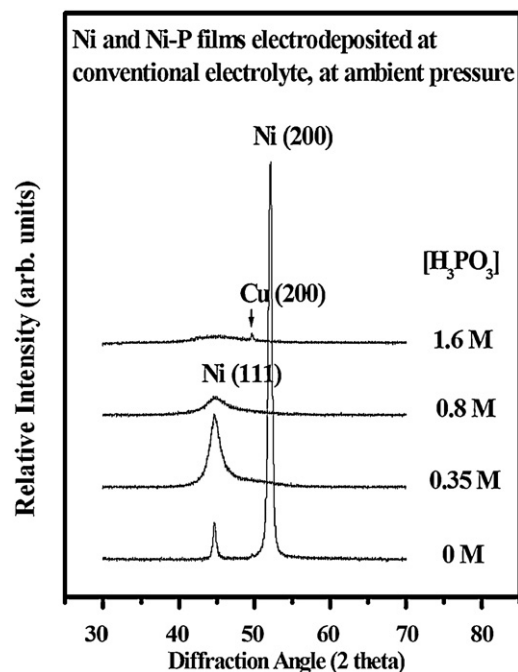


Fig. 5. X-ray diffraction patterns of the Ni deposit and Ni–P films electrodeposited in the conventional electrolyte with varying H_3PO_3 concentrations: 0.35 M, 0.8 M, and 1.6 M.

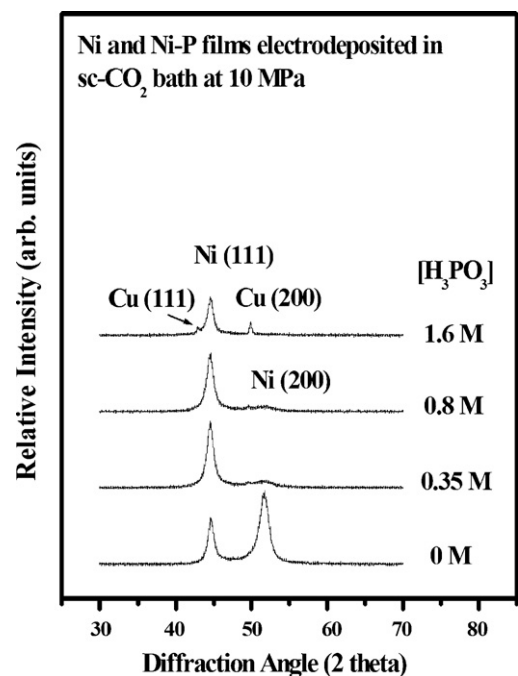


Fig. 6. X-ray diffraction patterns of the Ni deposit and Ni–P films electrodeposited in the emulsified sc- CO_2 bath at 10 MPa with varying H_3PO_3 concentrations: 0.35 M, 0.8 M, and 1.6 M.

distortion becomes large enough such that the crystalline phase cannot be maintained, and this leads to the formation of amorphous phase, as demonstrated in Fig. 5.

When electrodeposition was conducted in the emulsified sc- CO_2 containing electrolyte, a relatively weak dependence of crystallinity on H_3PO_3 concentration was observed, as depicted in Fig. 6. Although the change in preferred crystallographical plane from (200) to (111) was still observed with P alloying, the deposit still had a crystalline structure, even it was formed in the

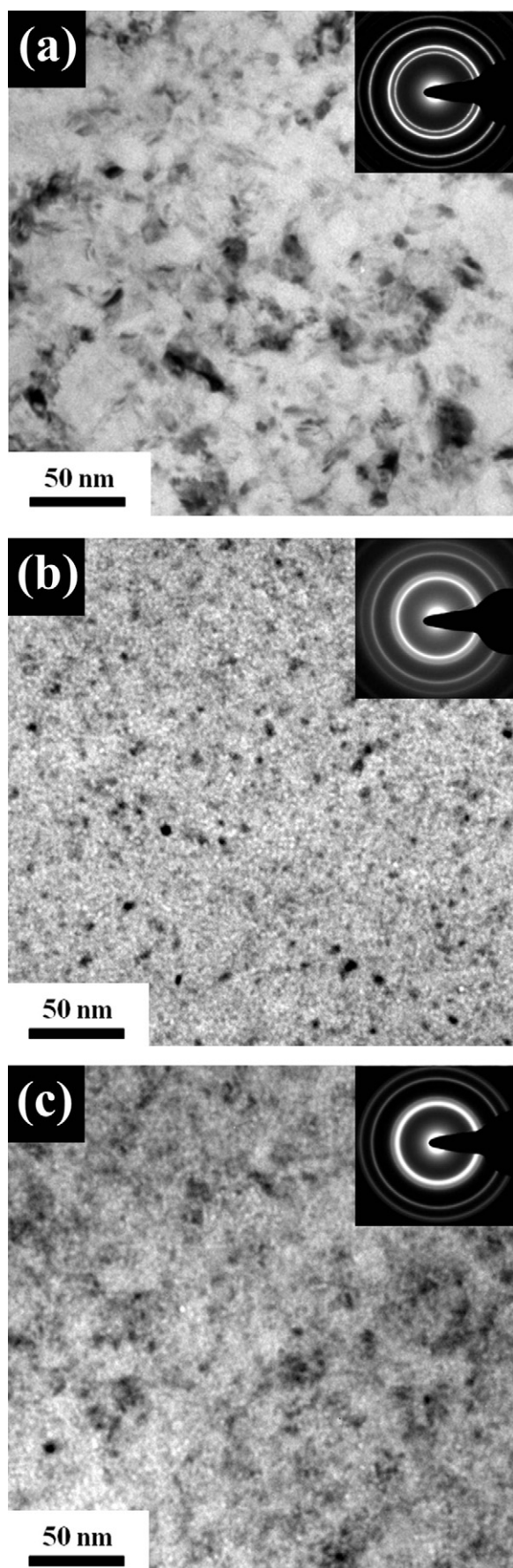


Fig. 7.

electrolyte containing 1.6 M H_3PO_3 . The lower P content in the Ni–P film deposited in the emulsified sc-CO_2 bath, as compared with that formed in the conventional electrolyte with the same H_3PO_3 concentration, was the main reason for the crystalline structure. However, a gradual decrease in diffraction peak intensity accompanied by a slight shift and widening of the Ni(1 1 1) peak was found when the concentration of H_3PO_3 in the emulsified sc-CO_2 bath was increased. A gradual decrease in grain size with increasing P content was expected, as confirmed by TEM analysis and discussed in the following section.

3.4. Microstructure

The TEM bright field images and the SAD patterns of the Ni–P coatings electrodeposited in conventional aqueous electrolyte at ambient pressure and in the emulsified sc-CO_2 bath are shown in Figs. 7 and 8, respectively. In both cases, the TEM images reveal that the deposits exhibited a nanocrystalline microstructure and the grain size became finer as the concentration of H_3PO_3 in both baths was increased. For the Ni–P film formed in conventional aqueous electrolyte, the grain size determined from the dark-field image decreased from 37 to 3 nm as the H_3PO_3 concentration was increased from 0.05 to 1.6 M. The decrease in average grain size of the Ni–P films was attributed to the increasing P content, as mentioned above. For the Ni–P films fabricated in the emulsified sc-CO_2 bath, the average grain size varied from 18 to 11 nm with increasing H_3PO_3 concentration from 0.05 to 1.6 M. The effect of sc-CO_2 in reducing the grain size of the deposit has been addressed by Yoshida et al. [18] and Chang et al. [25]. They reported that the “periodic” deposition characteristics in the emulsified sc-CO_2 bath, which affects the nucleation and grain growth behaviors, is the main factor leading to the grain size refinement. More specifically, the micelles formed in the emulsified bath contact the cathode surface in dynamic mode, which is similar to pulse plating. The on-and-off situation as appeared in pulse plating [36] retarding the crystal growth and leading to the formation of a fine crystalline nickel film. The TEM results were basically in agreement with those of the X-ray diffraction analyses. The grain sizes of the Ni–P alloys deposited either in the conventional bath and or in emulsified sc-CO_2 bath with different H_3PO_3 concentration are also listed in Table 2.

3.5. Hardness

A nanoindentation test was employed to determine the hardness of the electrodeposited Ni–P films. Fig. 9 shows the hardness of the Ni–P alloys with different P contents. The values of the P content and hardness of the various Ni–P films are summarized in Table 2. The hardness of pure Ni film formed at ambient pressure was measured as 5.2 GPa. P alloying caused a significant increase in the hardness of the Ni–P deposits. For the Ni–P films, the hardness increased with increasing P content to a peak of 10 GPa at about 9.7 at.% P, and then decreased afterwards.

Notably, a substantial increase in hardness to about 9.5 GPa was observed if pure Ni film was fabricated in the sc-CO_2 fluid containing bath. The significant increase in hardness was attributed to the fine grain size and solid solution strengthening from carbon, as reported previously [21]. For the Ni–P film electrodeposited in the sc-CO_2 bath, a higher hardness was observed as compared with that formed in the conventional bath with the same concentration of H_3PO_3 . The changes in crystallographical orientation and grain size associated with the alloying of P and C are responsible for the substantial increase in hardness.

According to Hall–Petch equation [37,38], the strength of a solid decreases linearly with the square root of grain size. Fig. 10 shows the Hall–Petch form of hardness vs. grain size relationship for Ni

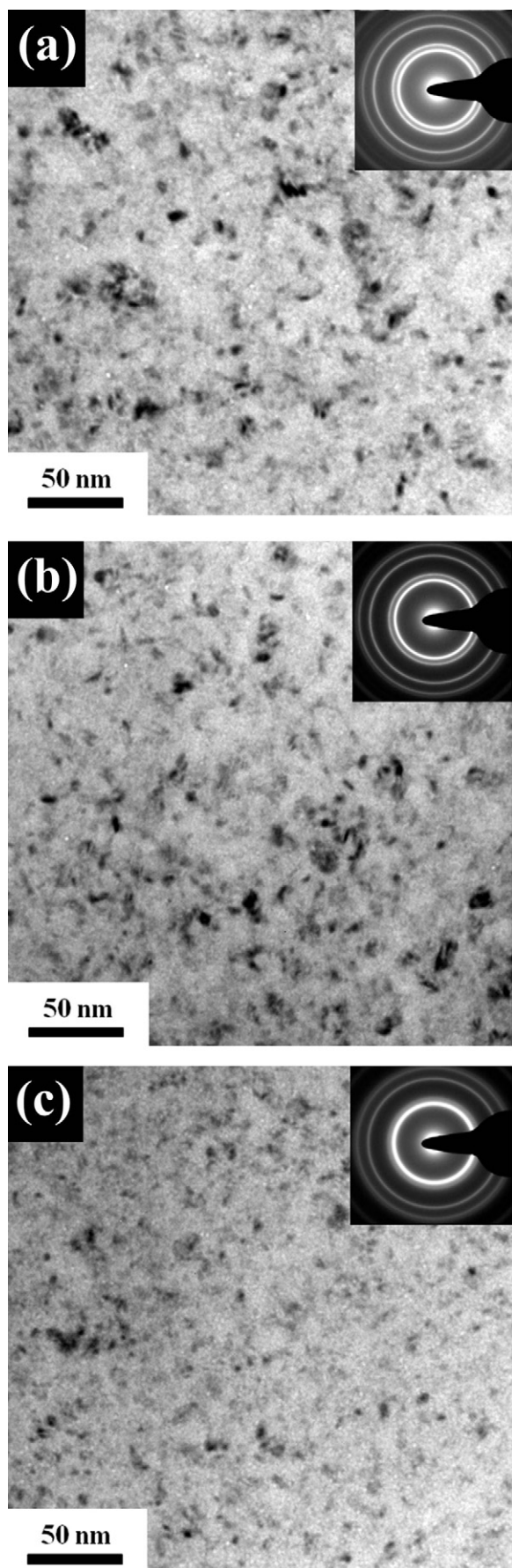


Fig. 8.

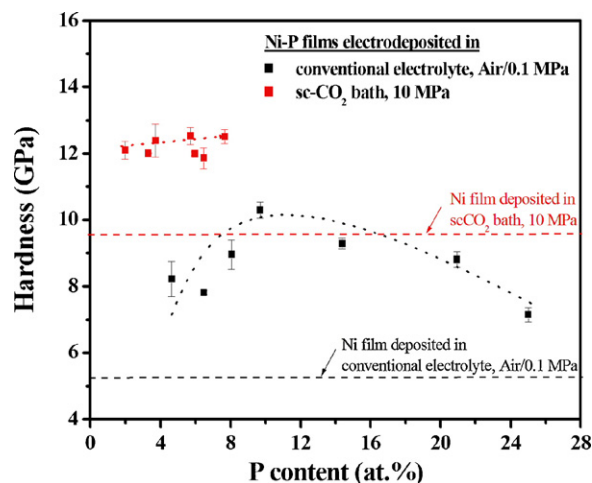


Fig. 9. Hardness of the Ni–P films electrodeposited at different P contents from conventional electrolyte at ambient pressure and in the emulsified sc-CO₂ bath at 10 MPa.

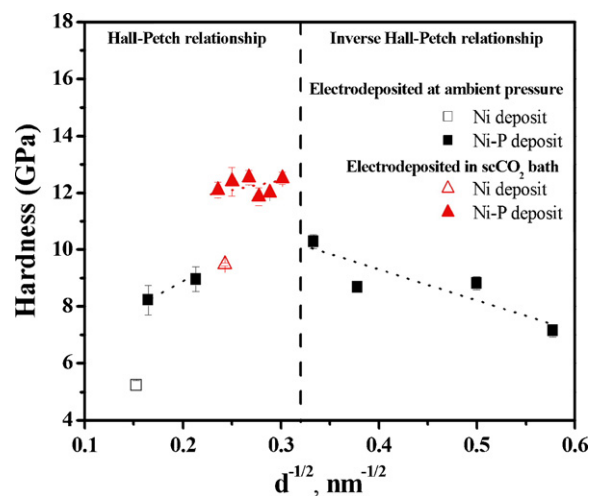


Fig. 10. Variation of hardness with grain size of various Ni and Ni–P films electrodeposited in the conventional and in the emulsified sc-CO₂ baths.

and Ni–P deposits with a P content less than 9.7 at.%. Obviously, the improvement in hardness of the Ni–P coatings is attributed to grain size strengthening. However, further increasing the P content beyond 9.7 at.% caused the hardness of the Ni–P deposits to decrease with decreasing grain size (see Table 2). For the Ni–P deposits with a higher P content (average grain size <10 nm), relaxation of atomic spacing and re-arrangement of atomic sites in the amorphous phase could render a low hardness, obeying the inverse Hall–Petch equation [39,40], namely

$$\sigma_y = \sigma_0 + (-k_y)d^{-1/2} \quad (3)$$

where σ_y is the tensile yield strength, σ_0 is the intrinsic stress resisting dislocation motion, and k_y is the proportional constant. Because the hardness of a material is generally proportional to its yield strength, the negative slope observed in Fig. 10 for the films with much finer grain size implies that the inverse Hall–Petch relationship is obeyed.

4. Conclusions

Co-deposition of Ni with P via electrodeposition could be performed in an emulsified sc-CO₂ bath. The P content in the Ni–P film, either deposited in a conventional or emulsified sc-CO₂ bath,

increased with increasing H_3PO_3 concentration, but with a sacrifice in current efficiency due to electron competition from H^+ and phosphorus oxyacid reductions. The weight gain of Ni and/or Ni–P film formed in the emulsified sc- CO_2 bath was lower than that found in the conventional bath, which was mainly attributed to the reduced number of active sites at the substrate/electrolyte interface for electrochemical reaction and the lower conductivity of the bath with the introduction of sc- CO_2 into the aqueous electrolyte. The Ni–P films deposited in the emulsified sc- CO_2 bath had a lower P content than that formed in the conventional bath with the same H_3PO_3 concentration. Electro-carburization of Ni and Ni–P film was found when electrodeposition was performed in the sc- CO_2 containing bath. Nanocrystalline microstructure was observed and the grain size of the deposit became finer as the P content in the deposit increased. Furthermore, the presence of sc- CO_2 in the electrodeposition bath enhanced the grain size refinement. A substantial increase in hardness of the Ni–P film was observed when it was fabricated in the emulsified sc- CO_2 bath. The changes in crystallographical orientation, grain size refinement and the alloying of P and C were responsible for the substantial increase in hardness of the Ni–P electrodeposits obtained.

Acknowledgement

The authors would like to thank the National Science Council of the Republic of China for supporting this study under Contract No. NSC 99-2622-E-006-011-CC1.

References

- [1] D.H. Jeong, U. Erb, K.T. Aust, G. Palumbo, *Scripta Mater.* 48 (2003) 1067.
- [2] M.H. Staia, E.J. Castillo, E.S. Puchi, B. Lewis, H.E. Hintermann, *Surf. Coat. Technol.* 86–87 (1996) 598.
- [3] G. Quercia, L. Grigorescu, H. Contreras, C.D. Rauso, D. Gutiérrez-Campos, *Int. J. Refract. Met. Hard Mater.* 19 (2001) 359.
- [4] J.L. Carbajal, R.E. White, *J. Electrochem. Soc.* 135 (1988) 2952.
- [5] G.J. Lu, G. Zangari, *Electrochim. Acta* 47 (2002) 2969.
- [6] P. Peeters, Gvd Hoorn, T. Daenen, A. Kurowski, G. Staikov, *Electrochim. Acta* 47 (2001) 161.
- [7] E. Bredael, B. Blanpain, J.P. Celis, J.R. Roos, *J. Electrochem. Soc.* 141 (1994) 294.
- [8] R.N. Duncan, *Plat. Surf. Finish.* 83 (1996) 65.
- [9] R.O. Scattergood, C.C. Koch, K.L. Murty, D. Brenner, *Mater. Sci. Eng. A* 493 (2008) 3.
- [10] M.H. Seo, J.S. Kim, W.S. Hwang, D.J. Kim, S.S. Hwang, B.S. Chun, *Surf. Coat. Technol.* 176 (2004) 135.
- [11] L. Chang, P.W. Kao, C.H. Chen, *Scripta Mater.* 56 (2007) 713.
- [12] T.M. Harris, Q.D. Dang, *J. Electrochem. Soc.* 140 (1993) 81.
- [13] E. Tóth-Kádár, I. Bakonyi, A. Sölyom, J. Hering, G. Konczos, F. Pavlyák, *Surf. Coat. Technol.* 31 (1987) 31.
- [14] R.L. Zeller III, U. Landau, *J. Electrochem. Soc.* 137 (1990) 1107.
- [15] J.W. Dini, H.R. Johnson, H.J. Saxton, *J. Vac. Sci. Technol.* 12 (1975) 766.
- [16] C.S. Lin, C.Y. Lee, F.J. Chen, W.C. Li, *J. Electrochem. Soc.* 152 (2005) C370.
- [17] H. Yoshida, M. Sone, A. Mizushima, K. Abe, X.T. Tao, S. Ichihara, S. Miyata, *Chem. Lett.* (2002) 1086.
- [18] H. Yoshida, M. Sone, H. Wakabayashi, K. Abe, X.T. Tao, A. Mizushima, H. Yan, S. Ichihara, S. Miyata, *Thin Solid Films* 446 (2004) 194.
- [19] K.M. Hong, M.S. Kim, J.G. Chung, *J. Ind. Eng. Chem.* 10 (2004) 683.
- [20] S.T. Chung, H.C. Huang, S.J. Pan, W.T. Tsai, P.Y. Lee, C.H. Yang, M.B. Wu, *Corros. Sci.* 50 (2008) 2614.
- [21] S.T. Chung, W.T. Tsai, *J. Electrochem. Soc.* 156 (11) (2009) D457.
- [22] S.T. Chung, W.T. Tsai, *Thin Solid Films* 518 (2010) 7236.
- [23] S.R.P. da Rocha, K.L. Harrison, K.P. Johnston, *Langmuir* 15 (1999) 419.
- [24] L. Lesoin, O. Boutin, C. Crampon, E. Badens, *Colloids Surf. A: Physicochem. Eng. Aspects* 377 (2011) 1.
- [25] T.F.M. Chang, M. Sone, A. Shibata, C. Ishiyama, Y. Higo, *Electrochim. Acta* 55 (2010) 6469.
- [26] M.S. Kim, J.Y. Kim, C.K. Kim, N.K. Kim, *Chemosphere* 58 (2005) 459.
- [27] E.D. Niemeyer, F.V. Bright, *J. Phys. Chem.* 102 (1998) 1474.
- [28] H.Y. Wang, S.T. Chung, Y.C. Chuang, W.T. Tsai, *Thin Solid Films* 518 (2010) 7236.
- [29] H. Uchiyama, A. Shibata, M. Sone, Y. Higo, *J. Electrochem. Soc.* 157 (2010) D550.
- [30] T.J. Moravec, T.W. Orent, *J. Vac. Sci. Technol.* 18 (2) (1981) 226.
- [31] A. Wiltner, Ch. Linsmeier, *Phys. Status Solidi A* 201 (2004) 881.
- [32] Gy.J. Kovács, I. Bertóti, G. Radnóczy, *Thin Solid Films* 516 (2008) 7942.
- [33] G. Li, Y.P. Gao, R.P. Liu, *J. Non-Cryst. Solids* 353 (2007) 4199.
- [34] J.W. Yeh, S.Y. Chang, Y.D. Hong, S.K. Chen, S.J. Lin, *Mater. Chem. Phys.* 103 (2007) 41.
- [35] P.S. Kumar, P.K. Nair, *J. Mater. Process. Technol.* 56 (1996) 511.
- [36] X. Yuan, Y. Wang, D. Sun, H. Yu, *Surf. Coat. Technol.* 202 (2008) 1895.
- [37] E.O. Hall, *Proc. Phys. Soc. Lond. Sect. B* 64 (1951) 747.
- [38] N.J. Petch, *J. Iron Steel Inst. (London)* 174 (1953) 25.
- [39] N. Wang, Z.R. Wang, K.T. Aust, U. Erb, *Acta Metall. Mater.* 43 (1995) 519.
- [40] H. Hahn, P. Mondal, K.A. Padmanabhan, *Nanostruct. Mater.* 9 (1997) 603.